MULTI-UNCERTAINTY AND MULTI-SCALE METHODS AND RELATED APPLICATIONS

EUROMECH 584 COLLOQUIUM

EUROMECH 584 COLLOQUIUM

Multi-uncertainty and multi-scale methods and related applications

September 14 - 16, 2016

Faculty of Engineering | University of Porto

Porto | Portugal

CHAIRPERSONS

Dr. F.M. Andrade Pires

Departament of Mechanical Engineering (DEMec)
Faculty of Engineering, University of Porto (FEUP)
Phone: +351 22 5083479,
fpires@fe.up.pt

Dr. Chenfeng Li

College of Engineering, Swansea University
Phone: +44 (1792) 602256,
c.f.li@swansea.ac.uk

LOCAL ORGANIZING COMMITTEE

Carla Monteiro

Departament of Mechanical Engineering (DEMec)
Faculty of Engineering, University of Porto (FEUP)
monteiro@fe.up.pt

Dr. Mohsen Mirkhalaf

Departament of Mechanical Engineering (DEMec)
Faculty of Engineering, University of Porto (FEUP)
Email: moshen.mirkhalaf@fe.up.pt

Dr. Shenghua Wu

Departament of Mechanical Engineering (DEMec)
Faculty of Engineering, University of Porto (FEUP)
Email: shenghua@fe.up.pt

Connect your mobile device to the **UPorto** wifi network.

Open a browser and enter the portal to the following credentials:

Username: **euromech**

Password: **584colloquium**

Shelf life: **2016-09-13** the **2016-09-17**

In case of doubt contact the helpdesk service:

helpdesk@uporto.pt

MULTI-UNCERTAINTY AND MULTI-SCALE METHODS AND RELATED APPLICATIONS

Wednesday, September 14

Room B032

	MORNING
08:30 – 09:00	*Registration and check-in*
09:00 – 09:30	*Welcome Remarks*
09:30 –10:30	Plenary Session: **Marc Geers** | Eindhoven University of Technology | ***Modeling of interfaces in engineering materials across the scales***
10:30 – 10:50	**Chris Pearce** | University of Glasgow | ***Nonlinear micro-mechanical response of fibre-reinforced polymer composites including matrix damage and fibre-matrix decohesion***
10:50 – 11:10	**George Stefanou** | Dept. of Civil Engineering , Aristotle University of Thessaloniki | ***Determination of the apparent properties and RVE size of spatially random composites***
11:10 – 11:40	*Coffee Break*
11:40 – 12:00	**Jacek Ptaszny** | Institute of Computational Mechanics and Engineering, Silesian University of Technology, Poland | ***Evaluation of the fast multipole boundary element method efficiency in numerical homogenization***
12:00 – 12:20	**Wengang Zhang** | School of Civil Engineering, Chongqing University, China | ***Probabilistic assessment of serviceability limit state of diaphragm walls for braced excavation using mars_mcs***
12:20 – 12:40	**Wolfgang Graf** | Technische Universität Dresden | ***Numerical structural design concepts with polymorphic uncertain data***
12:40 – 13:00	**Abdibekova Aigerim** | Al-Farabi Kazakh National University | ***Modelling of turbulence energy decay based on hybrid methods***
13:00 – 14:00	*Lunch*

Wednesday, September 14

Room B032

	AFTERNOON
14:00 – 15:00	Plenary Session: **J. Oliver** | Technical University of Catalonia (UPC/Barcelona Tech) International Center for Numerical Methods in Engineering (CIMNE), Barcelona, Spain| ***Hyper-reduced order modelling (HPROM) in multiscale fracture***
15:00 – 15:20	**Caglar Oskay** | Vanderbilt University | ***Accelerated reduced order homogenization of polycrystal plasticity***
15:20 – 15:40	**Claudia Brito de Carvalho Bello** | Department of Architecture Construction Conservation, Università IUAV di Venezia | ***Experimental on three-leaf brick masonry walls: the scale factor***
15:40 – 16:00	**Duanzhong Zhang** | Los Alamos National Laboratory | ***Multiscale formulation implemented using the dual domain material point method***
16:00 – 16:20	**Liu Liu** | Institute of Natural Sciences, Department of Mathematics Shanghai Jiao Tong University, Shanghai and Department of Mathematics, University of Wisconsin | ***An asymptotic-preserving stochastic Galerkin method for the semiconductor Boltzmann equation with random inputs and diffusive scalings***
16:20 – 17:20	Plenary Session: **Michael Beer** | Institute for Risk and Reliability, Leibniz University Hannover, Germany; Institute for Risk and Uncertainty, University of Liverpool, United Kingdom; Shanghai Institute of Disaster Prevention and Relief, Tongji University, China | ***Coherent Models for Aleatory and Epistemic Uncertainties***
17:20	*Departure from FEUP*
17:30	*Welcome Cocktail @Reitoria*

MULTI-UNCERTAINTY AND MULTI-SCALE METHODS AND RELATED APPLICATIONS

Thursday, September 15

Room B032

	MORNING
09:00 – 10:00	Plenary Session: **Wing K. Liu**| Northwestern University| ***Modeling and Simulation Challenges in Materials Design for Additive Manufacturing Applications***
10:00 – 10:20	**Niraj Kumar Jha** | Leibniz University Hannover | ***Fatigue life prediction of composite structures based on progressive damage analysis***
10:20 – 10:40	**Saida Dorbani** | Built Environment Lab. (LBE), Faculty of Civil Engineering, University of Sciences and Technologies Houari Boumediene, Algiers, Algeria |***The seismic behavior of RC buildings with uncertain natural period and epicentral distance***
10:40 – 11:10	*Coffee Break*
11:10 – 11:50	Plenary Session: **Ron Bates** | Rolls Royce plc |***Multi-Scale Robust Design for Product Development***
11:50 – 12:10	**Yoshihiro Kanno** | Tokyo Institute of Technology Japan | ***Redundancy optimization of trusses against uncertainty in structural damage***
12:10 – 12:30	**Shaoqing Cui** | Zienkiewicz Centre for Computational Engineering, College of Engineering, Swansea University | ***Stochastic reconstruction of heterogeneous media***
12:30 – 12:50	**Shi Jin** | University of Wisconsin-Madison | ***Uncertainty quantification for multiscale hyperbolic and kinetic equations with uncertain coefficients***
12:50 – 14:00	*Lunch*

Thursday, September 15

Room B032

	AFTERNOON
14:00 – 15:00	Plenary Session: **M.Papadrakakis** | Institute of Structural Analysis & Antiseismic Research - National Technical University Athens, Greece| ***High Performance Methods for Non-Intrusive and Intrusive Multiscale Stochastic Simulations***
15:00 –15:20	**Srihari Dodla** | WolfsonSchool of Mechanical, Electrical and Manufacturing Engineering, Loughborough University | ***Finite element simulations of plastic deformation behavior of textured ti64***
15:20 – 15:40	**Jouni Freund** | Aalto University, School of Engineering, Finland| ***Two-scale modelling of layered plates***
15:40 – 16:00	**Deepanshu Sodhani** | Institute of Applied Mechanics, RWTH Aachen University | ***Artificial textile reinforced tubular aortic heart valves -multi-scale modelling and experimental validation***
16:00 – 16:30	*Coffee Break*
16:30 – 16:50	**Jie Yuan** | Aerospace Division, Cranfield University; Airbus Operations Ltd, Bristol; Aerospace Engineering, University of Bristol | ***A framework of computational reduction techniques for probabilistic margin assessment in aircraft design***
16:50 – 17:10	**Alena A. Ayzenberg** | University of Bergen | ***Tpot & twsm for 3d multiphysics multi–scale models with complex interfaces. Uu-model solution separation***
17:10 – 17:30	**João Cardoso** | UNIDEMI, Dep. Mechanical and Industrial Eng, FCT/UNL, Portugal | ***Structural optimization of composite laminates including uncertainty***
17:30 – 17:50	**Fermin Otero** | Institute of Science and Innovation in Mechanical and Industrial Engineering (INEGI) | ***Efficient multi-scale strategy for material non-linear analysis through a computational homogenization***
17:50 – 18:50	Discussion Panel
19:00	*Departure from FEUP*
20:00	*Conference Banquet @ Cálem Port Wine Cellar*

MULTI-UNCERTAINTY AND MULTI-SCALE METHODS AND RELATED APPLICATIONS

Friday, September 16

Room B032

	MORNING
09:00 – 09:20	**Jan Chleboun** | Faculty of Civil Engineering, Czech Technical University in Prague | ***A fuzzy set approach to uncertain functions***
09:20 – 09:40	**Thanusha M.T** | Indian Institute of Technology,Madras | ***Optimum sampling technique for subcritical nonlinear aeroelastic system with discontinuous response surface***
09:40 – 10:20	**Pedro Coelho** | UNIDEMI, Universidade Nova de Lisboa | ***Laminates with fibre lay-out and lay-up sequence optimized for stiffness via multiscale topology optimization***
10:20 – 10:40	**Ashutosh Gandhi** | Institute of Mechanics and Shell Structures, TU Dresden, Germany| ***Influence of microstructure morphology on multi-scale modeling of low-alloyed TRIP steels***
10:40 – 11:10	*Coffee Break*
11:10 – 11:30	**José Reinoso-Cuevas** | Elasticity and Strength of Materials Group, School of Engineering, University of Seville | ***Delamination of structured interfaces using a novel anisotropic cohesive interface formulation***
11:30 – 11:50	**Igor Lopes** | Department of Mechanical Engineering, Faculty of Engineering, University of Porto | ***A mixed parallel strategy for the solution of homogenization-based multi-scale problems***
11:50 – 12:10	**Dimitrios Savvas** | School of Civil Engineering, National Technical University of Athens | ***Homogenization of two-phase composites with random material properties***
12:10 – 12:30	**Ramin Mirzazadeh** | Politecnico di Milano, Department of Civil and Environmental Engineering | ***Uncertainty quantification of the micro-mechanical properties of polysilicon films***
12:30 – 12:50	**Rodrigo Carvalho** | Department of Mechanical Engineering, Faculty of Engineering, University of Porto | ***Yielding behaviour of anisotropic porous materials through computational homogenization***
12:50 – 14:00	*Lunch*

Friday, September 16

Room B032

	AFTERNOON
14:00 – 15:00	Plenary Session: **Souza Neto** | Civil Engineering College of Engineering Swansea University | ***The Method of Multiscale Virtual Power. A Variational Recipe for Derivation of RVE-based Multiscale Models***
15:00 – 15:20	**Daniel de Bortoli** | Swansea University Zienkiewicz Centre for Computational Engineering | ***Multi-scale modelling of stress-induced martensitic transformations***
15:20 – 15:40	**Ielizaveta Khometska** | Czech Technical University in Prague, Faculty of Civil Engineering | ***Uncertainty in the modeling of magnetostrictive materials and magnetostrictive energy harvesters***
15:40 – 16:00	**Thiago Doca** | University of Brasilia | ***Assessment of a contact homogenization method for the analysis of abrasive wear problems***
16:00 – 16:20	**Alena A. Ayzenberg** | University of Bergen | ***Generalized Lippmann-Schwinger equation for initial boundary value problem in 3d blocky multiphysics multi-scale media***
16:20 – 16:40	**Muhannad Aldosary** | Swansea University | ***Structural reliability analysis- a review and comparison study***
16:40 – 17:00	*Coffee Break*
17:20	Closing Remarks

MODELLING OF TURBULENCE ENERGY DECAY BASED ON HYBRID METHODS

[1]Abdibekova A.U., [2]Zhakebayev D.B., [3]Zhubatov Zh.

[1 2]Al-Farabi Kazakh National University, [1]a_aigerim@inbox.ru, [2]daurjaz@mail.ru

[3]Scientific-Research Center «Garysh-Ecology», infracos-kaz@mail.ru

Abstract

Purpose

The purpose of this paper is to present an exact and fast calculated algorithm based on two different methods: finite-difference and spectral methods for modelling of turbulent energy decay.

Design/Methodology/approach

The filtered three-dimensional non-stationary Navier-Stokes equation is used for simulation the turbulent process. The problem is solved by using hybrid methods, where the equation of motion is solved by using finite-difference methods in combination with cyclic penta-diagonal matrix, which allowed to reach high order of accuracy and Poisson equation is solved by using the spectral methods, which is proposed to speed up the solution procedure. For validation of the given algorithm the turbulent characteristics were compared with the exact solution of classical problem of Taylor and Green vortex and showed good agreements.

Findings

It shows high computational efficiency and good estimation quality.

The numerical algorithm of solving non-stationary three-dimensional Navier-Stokes equations for modelling of isotropic turbulence decay with using hybrid methods was developed. The numerical simulation results in obtaining turbulence characteristics show good agreements with analytical solution. The developed numerical algorithm can be used for simulation of the turbulence decay at the different properties of the viscosity.

Originality/value

The efficient algorithm for simulation turbulence process depending on the properties of the viscosity was developed.

Keywords: Taylor –Green vortex, turbulence decay, cyclic penta-diagonal matrix.

Introduction

Rapidly developing computing technologies and new software packages are proposing more requirements to the modeling of physical processes to obtain the corresponding actual physical paintings and the most accurate results. The problem solutions of hydrodynamics, magnetohydrodynamics and other areas with enough large system of equations with special boundary conditions are encountered, that take a long time for calculations, where at times the solution may be unsatisfactory. Thereby, the construction of sufficiently flexible, high-speed and high-precision algorithms for computer calculations is an urgent problem.

In the solution was suggested using classical example proposed by Taylor and Green. Taylor-Green vortex combinations of words have come into sight after presentation of the work [1], first published a method for successive approximations to formula

describing three dimensional turbulence evolution over time. There was considered the decay of three dimensional turbulence flow produced in wind tunnel, where was represented the effect of the fundamental process in turbulent flow, to wit, the grinding down of eddies, produced by solid obstructions. In result the kinetic energy and the dissipation rate of turbulent decay were defined analytically.

Many works of the Taylor-Green vortex problem investigated from the numerical side. One of them was referred in [2], where the Taylor- Green vortex problem was studied by two methods: spectral numerical solution and power-series analysis in time computed. In the result of simulation the energy simulation and spectra energy at different Reynolds number were presented and compared. Later, in [3] three dimensional Navier –Stockes equations was numerically integrated with setting periodic Taylor-Green initial condition and simulated at high Reynolds numbers. In the direct numerically simulation result the slope of energy spectrum was compared with 5/3 Kolmogorov's value. Moreover, compressible Navier-Stockes equation was applied to the Taylor-Green vortex problem [4] with using wave resolving large eddy simulation. Numerical scheme investigations were setting up at different resolution of grid. Eventually, the dissipation rate of kinetic energy and evolution of kinetic energy were compared at different grid size. However, in all these observed work the comparison results of turbulent characteristics, such as dissipation rate and kinetic energy with exact analytically solution were not fully reflected.

This work deals with the modelling of turbulent energy decay using two methods: finite-difference and spectral methods. To simulate the turbulent process the filtered three-dimensional non-stationary Navier-Stokes equation is used. The problem is solved by using hybrid methods, where the equation of motion is solved by using finite-difference methods in combination with cyclic penta-diagonal matrix, which allowed to reach high order of accuracy and to simulate turbulence decay at high Reynolds number $\mathrm{Re} = 10^4$, and spectral methods is used for solution of Poisson equation, which is makes it possible to gain the time. For validation of the given algorithm the classical problem of Taylor and Green for modeling of isotropic turbulence decay was solved.

Analitical solution of Taylor-Green vortex problem

We duplicate classical example proposed by [1] to reconsider through use of numerical simulation for increasing the order of accuracy in time and in space $O(t^3, h^4)$ and also to getting efficient acceleration for sequential algorithm. Starting from a simple incompressible three-dimensional initial condition of the form

$$u_1(x_1, x_2, x_3, t = 0) = \cos(ax_1)\sin(ax_2)\sin(ax_3),$$
$$u_2(x_1, x_2, x_3, t = 0) = -\sin(ax_1)\cos(ax_2)\sin(ax_3),$$
$$u_3(x_1, x_2, x_3, t = 0) = 0.$$

and assuming periodic conditions in a cubic domain: $0 \le x_1 \le 2\pi$, $0 \le x_2 \le 2\pi$, $0 \le x_3 \le 2\pi$, the three dimensional Navier-Stokes equation

$$\frac{\partial u_i}{\partial t} + u_j \frac{\partial u_i}{\partial x_j} = -\frac{\partial p}{\partial x_i} + \frac{1}{\mathrm{Re}} \frac{\partial^2 u_i}{\partial x_i \partial x_j} \tag{1}$$

can be solved analitically at small times, using petrubation expansion. At (1) all quantities have been proparly normalized by the initial maximum velosity magnitude U_0 in the x_1 or x_2 direction, and $L/2\pi$, where L is the physical domain size, u_i -velocity at $i = 1, 2, 3$, corresponding to x_1, x_2, x_3 directions, $\mathrm{Re} = LU_0/v$ is the Reynolds number of flow, U_0 - the characteristic velocity, $T = aU_0 t, a = 2\pi/L.$ The pressure p has been normalized by ρU_0^2 .

Taylor Green obtained petrubation expansion of the velocity field, up to $O(t^5)$. The kinetic energy equation is looks like:

$$E_k = \frac{U_0^2}{8} u'^2$$

where

$$u'^2 = 1 - \frac{6T}{\mathrm{Re}} + \frac{18T^2}{\mathrm{Re}^2} - \left(\frac{5}{24} + \frac{36}{\mathrm{Re}^2}\right)\frac{T^3}{\mathrm{Re}} + \left(\frac{5}{2\,\mathrm{Re}^2} + \frac{54}{\mathrm{Re}^4}\right)T^4 -$$
$$- \left(\frac{5}{44.12} + \frac{367}{24\,\mathrm{Re}^2} + \frac{4.81}{5\,\mathrm{Re}^4}\right)\frac{T^5}{\mathrm{Re}} + \left(\frac{361}{44.32} + \frac{761}{12\,\mathrm{Re}^2} + \frac{324}{5\,\mathrm{Re}^4}\right)\frac{T^6}{\mathrm{Re}^2}.$$

The dissipation rate is writing in the following form:

$$W = \mu \frac{3U_0^2 a^2}{4} W'$$

where

$$W' = 1 - \frac{6T}{\mathrm{Re}} + \left(\frac{5}{48} + \frac{18}{\mathrm{Re}^2}\right)T^2 - \left(\frac{5}{3} + \frac{36}{\mathrm{Re}^2}\right)\frac{T^3}{\mathrm{Re}} +$$
$$+ \left(\frac{50}{99.64} + \frac{1835}{9.16\,\mathrm{Re}^2} + \frac{54}{\mathrm{Re}^4}\right)T^4 - \left(\frac{361}{44.32} + \frac{761}{12\,\mathrm{Re}^2} + \frac{324}{5\,\mathrm{Re}^4}\right)\frac{T^5}{\mathrm{Re}}.$$

Numerical solution of Taylor-Green vortex problem

In this paper a three-dimensional non-stationary Navier-Stokes equation is solved for modelling of isotropic turbulence decay. For solving the Navier–Stokes equation, we use a splitting scheme by physical parameters that consists of three stages of Adams Bashforth method [5].

At the first stage, the equation for motion is solved, without taking pressure into the account. For approximation of the convective and diffusion terms of the intermediate velocity field the finite-difference methods in combination with cyclic penta-diagonal matrix is used [6], which allowed to increase the order of accuracy in time and in space $O(t^3, h^4)$ without changing the amount of points.

The intermediate velocity field is solved by using the Adams Bashforth scheme in combination with a five-point sweep method.
Lets considered the horizontal component of the velocity u_1 components in the point of grid $(i+\frac{1}{2}\,jk)$:

$$\frac{\partial u_1}{\partial \tau}+\frac{\partial(u_1u_1)}{\partial x_1}+\frac{\partial(u_1u_2)}{\partial x_2}+\frac{\partial(u_1u_3)}{\partial x_3}=\frac{1}{\mathrm{Re}}\left(\frac{\partial^2 u_1}{\partial x_1^2}+\frac{\partial^2 u_1}{\partial x_2^2}+\frac{\partial^2 u_1}{\partial x_3^2}\right) \tag{2}$$

In the application of the scheme Adams Bashforth equation (2) takes the form:

$$\hat{u}_{1}{}^{n+1}_{i+\frac{1}{2}jk}-u_{1}{}^{n}_{i+\frac{1}{2}jk}=-\frac{3\tau}{2}\left[hx\right]^{n}_{i+\frac{1}{2}jk}+\frac{\tau}{2}\left[hxp\right]^{n-1}_{i+\frac{1}{2}jk}+\tau\left[ax\right]^{n}_{i+\frac{1}{2}jk}$$
$$+\frac{\tau}{2}\cdot\frac{1}{\mathrm{Re}}\cdot\left(\frac{\partial^2\hat{u}_1}{\partial x_1^2}\right)^{n+1}_{i+\frac{1}{2}jk}+\frac{\tau}{2}\cdot\frac{1}{\mathrm{Re}}\cdot\left(\frac{\partial^2\hat{u}_1}{\partial x_2^2}\right)^{n+1}_{i+\frac{1}{2}jk}+\frac{\tau}{2}\cdot\frac{1}{\mathrm{Re}}\cdot\left(\frac{\partial^2\hat{u}_1}{\partial x_3^2}\right)^{n+1}_{i+\frac{1}{2}jk} \tag{3}$$

where

$$\left[hx\right]^{n}_{i+\frac{1}{2}jk}=\left(\frac{\partial u_1u_1}{\partial x_1}\right)^{n}_{i+\frac{1}{2}jk}+\left(\frac{\partial u_1u_2}{\partial x_2}\right)^{n}_{i+\frac{1}{2}jk}+\left(\frac{\partial u_1u_3}{\partial x_3}\right)^{n}_{i+\frac{1}{2}jk}$$
$$\left[hxp\right]^{n-1}_{i+\frac{1}{2}jk}=\left(\frac{\partial u_1u_1}{\partial x_1}\right)^{n-1}_{i+\frac{1}{2}jk}+\left(\frac{\partial u_1u_2}{\partial x_2}\right)^{n-1}_{i+\frac{1}{2}jk}+\left(\frac{\partial u_1u_3}{\partial x_3}\right)^{n-1}_{i+\frac{1}{2}jk}$$
$$\left[ax\right]^{n}_{i+\frac{1}{2}jk}=\frac{1}{2}\cdot\frac{1}{\mathrm{Re}}\cdot\left[\left(\frac{\partial^2 u_1}{\partial x_1^2}\right)^{n}_{i+\frac{1}{2}jk}+\left(\frac{\partial^2 u_1}{\partial x_2^2}\right)^{n}_{i+\frac{1}{2}jk}+\left(\frac{\partial^2 u_1}{\partial x_3^2}\right)^{n}_{i+\frac{1}{2}jk}\right]$$

Then the left side of equation (3) is denoted by $q_{i+\frac{1}{2}jk}$

$$q_{i+\frac{1}{2}jk}\equiv\hat{u}_{1}{}^{n+1}_{i+\frac{1}{2}jk}-u_{1}{}^{n}_{i+\frac{1}{2}jk} \tag{4}$$

We find $\hat{u}_{1}{}^{n+1}_{i+\frac{1}{2}jk}$ from the equation (4)

$$\hat{u}_{1}{}^{n+1}_{i+\frac{1}{2}jk}=q_{i+\frac{1}{2}jk}+u_{1}{}^{n}_{i+\frac{1}{2}jk}$$

Replacing all $\hat{u}_{1}{}^{n+1}_{i+\frac{1}{2}jk}$ from the equations (3) we obtain

$$q_{i+\frac{1}{2}jk} - \frac{\tau}{2}\cdot\frac{1}{\mathrm{Re}}\cdot\left(\frac{\partial^2 q}{\partial x_1^2}\right)^{n+1}_{i+\frac{1}{2}jk} - \frac{\tau}{2}\cdot\frac{1}{\mathrm{Re}}\cdot\left(\frac{\partial^2 q}{\partial x_2^2}\right)^{n+1}_{i+\frac{1}{2}jk} - \frac{\tau}{2}\cdot\frac{1}{\mathrm{Re}}\cdot\left(\frac{\partial^2 q}{\partial x_3^2}\right)^{n+1}_{i+\frac{1}{2}jk} = \\ = -\frac{3\tau}{2}[hx]^{n}_{i+\frac{1}{2}jk} + \frac{\tau}{2}[hxp]^{n-1}_{i+\frac{1}{2}jk} + 2\cdot\tau[ax]^{n}_{i+\frac{1}{2}jk} \tag{5}$$

We present the equation (5) in view of

$$\left[1-\frac{\tau}{2}\cdot\frac{1}{\mathrm{Re}}\cdot\frac{\partial^2}{\partial x_1^2}-\frac{\tau}{2}\cdot\frac{1}{\mathrm{Re}}\cdot\frac{\partial^2}{\partial x_2^2}-\frac{\tau}{2}\cdot\frac{1}{\mathrm{Re}}\cdot\frac{\partial^2}{\partial x_3^2}\right]q_{i+\frac{1}{2}jk} = d_{i+\frac{1}{2}jk} \tag{6}$$

where $d_{i+\frac{1}{2}jk} = -\frac{3\tau}{2}[hx]^{n}_{i+\frac{1}{2}jk} + \frac{\tau}{2}[hxp]^{n-1}_{i+\frac{1}{2}jk} + 2\cdot\tau[ax]^{n}_{i+\frac{1}{2}jk}$

To obtain the second order of accuracy with respect to time, we will solve the following equation:

$$\left[1-\frac{\tau}{2}\cdot\frac{1}{\mathrm{Re}}\cdot\frac{\partial^2}{\partial x_1^2}\right]\left[1-\frac{\tau}{2}\cdot\frac{1}{\mathrm{Re}}\cdot\frac{\partial^2}{\partial x_2^2}\right]\left[1-\frac{\tau}{2}\cdot\frac{1}{\mathrm{Re}}\cdot\frac{\partial^2}{\partial x_3^2}\right]q_{i+\frac{1}{2}jk} = d_{i+\frac{1}{2}jk} \tag{7}$$

To determine $q_{i+\frac{1}{2}jk}$ the equation (7) is solved in 3 stages.

$$\left[1-\frac{\tau}{2}\cdot\frac{1}{\mathrm{Re}}\cdot\frac{\partial^2}{\partial x_1^2}\right]A_{i+\frac{1}{2}jk} = d_{i+\frac{1}{2}jk}$$
$$\left[1-\frac{\tau}{2}\cdot\frac{1}{\mathrm{Re}}\cdot\frac{\partial^2}{\partial x_2^2}\right]B_{i+\frac{1}{2}jk} = A_{i+\frac{1}{2}jk}$$
$$\left[1-\frac{\tau}{2}\cdot\frac{1}{\mathrm{Re}}\cdot\frac{\partial^2}{\partial x_3^2}\right]q_{i+\frac{1}{2}jk} = B_{i+\frac{1}{2}jk}$$

At the first stage $A_{i+\frac{1}{2}jk}$ sought in the direction coordinates x_1:

$$\left[1-\frac{\tau}{2}\cdot\frac{1}{\mathrm{Re}}\cdot\frac{\partial^2}{\partial x_1^2}\right]A_{i+\frac{1}{2}jk} = d_{i+\frac{1}{2}jk}$$

$$A^{n+1}_{i+\frac{1}{2}jk} - \frac{\tau}{2}\cdot\frac{1}{\mathrm{Re}}\cdot\left(\frac{\partial^2 A}{\partial x_1^2}\right)^{n+1}_{i+\frac{1}{2}jk} = d_{i+\frac{1}{2}jk}$$

$$A^{n+1}_{i+\frac{1}{2}jk} - \frac{\tau}{2}\cdot\frac{1}{\mathrm{Re}}\cdot\frac{-A^{n+1}_{i+\frac{5}{2}jk}+16\cdot A^{n+1}_{i+\frac{3}{2}jk}-30\cdot A^{n+1}_{i+\frac{1}{2}jk}+16\cdot A^{n+1}_{i-\frac{1}{2}jk}-A^{n+1}_{i-\frac{3}{2}jk}}{12\Delta x_1^2} = d_{i+\frac{1}{2}jk}$$

$$s_1 \cdot A^{n+1}_{i+\frac{5}{2}jk} - 16 \cdot s_1 \cdot A^{n+1}_{i+\frac{3}{2}jk} + \left(1 + 30 \cdot s_1\right) \cdot A^{n+1}_{i+\frac{1}{2}jk} - 16 \cdot s_1 \cdot A^{n+1}_{i-\frac{1}{2}jk} + s_1 \cdot A^{n+1}_{i-\frac{3}{2}jk} = d_{i+\frac{1}{2}jk} \qquad (8)$$

where $s_1 = \dfrac{\tau}{24 \cdot \mathrm{Re} \cdot \Delta x_1^2}$

This equation (8) is solved by the cyclic penta - diagonal matrix method, the result of which the $A^{n+1}_{i+\frac{1}{2}jk}$ is defined.

The second stage $B_{i+\frac{1}{2}jk}$ is looked in the direction of the coordinates x_2:

$$\left[1 - \frac{\tau}{2} \cdot \frac{1}{\mathrm{Re}} \cdot \frac{\partial^2}{\partial x_2^2}\right] B_{i+\frac{1}{2}jk} = A_{i+\frac{1}{2}jk}$$

$$B^{n+1}_{i+\frac{1}{2}jk} - \frac{\tau}{2} \cdot \frac{1}{\mathrm{Re}} \cdot \left(\frac{\partial^2 B}{\partial x_2^2}\right)^{n+1}_{i+\frac{1}{2}jk} = A^{n+1}_{i+\frac{1}{2}jk}$$

$$B^{n+1}_{i+\frac{1}{2}jk} - \frac{\tau}{2} \cdot \frac{1}{\mathrm{Re}} \cdot \frac{-B^{n+1}_{i+\frac{1}{2}j+2k} + 16 \cdot B^{n+1}_{i+\frac{1}{2}j+1k} - 30 \cdot B^{n+1}_{i+\frac{1}{2}jk} + 16 \cdot B^{n+1}_{i+\frac{1}{2}j-1k} - B^{n+1}_{i+\frac{1}{2}j-2k}}{12\Delta x_2^2} = A^{n+1}_{i+\frac{1}{2}jk}$$

$$\begin{aligned} &s_2 \cdot B^{n+1}_{i+\frac{1}{2}j+2k} - 16 \cdot s_2 \cdot B^{n+1}_{i+\frac{1}{2}j+1k} + \left(1 + 30 \cdot s_2\right) \cdot B^{n+1}_{i+\frac{1}{2}jk} - \\ &- 16 \cdot s_2 \cdot B^{n+1}_{i+\frac{1}{2}j-1k} + s_2 \cdot B^{n+1}_{i+\frac{1}{2}j-2k} = A^{n+1}_{i+\frac{1}{2}jk} \end{aligned} \qquad (9)$$

where $s_2 = \dfrac{\tau}{24 \cdot \mathrm{Re} \cdot \Delta x_2^2}$

This equation (9) is solved by cyclic penta - diagonal matrix method, as a result of which the $B^{n+1}_{i+\frac{1}{2}jk}$ is defined.

At the third stage $q_{i+\frac{1}{2}jk}$ is sought in the direction of the coordinates x_3:

$$\left[1 - \frac{\tau}{2} \cdot \frac{1}{\mathrm{Re}} \cdot \frac{\partial^2}{\partial x_3^2}\right] q_{i+\frac{1}{2}jk} = B_{i+\frac{1}{2}jk}$$

$$q^{n+1}_{i+\frac{1}{2}jk} - \frac{\tau}{2} \cdot \frac{1}{\mathrm{Re}} \cdot \left(\frac{\partial^2 q}{\partial x_3^2}\right)^{n+1}_{i+\frac{1}{2}jk} = B_{i+\frac{1}{2}jk}$$

$$q^{n+1}_{i+\frac{1}{2}jk} - \frac{\tau}{2} \cdot \frac{1}{\mathrm{Re}} \cdot \frac{-q^{n+1}_{i+\frac{1}{2}j+2k} + 16 \cdot q^{n+1}_{i+\frac{1}{2}j+1k} - 30 \cdot q^{n+1}_{i+\frac{1}{2}jk} + 16 \cdot q^{n+1}_{i+\frac{1}{2}j-1k} - q^{n+1}_{i+\frac{1}{2}j-2k}}{12\Delta x_3^2} = B^{n+1}_{i+\frac{1}{2}jk}$$

$$s_3 \cdot q^{n+1}_{i+\frac{1}{2}j+2k} - 16 \cdot s_3 \cdot q^{n+1}_{i+\frac{1}{2}j+1k} + (1+30 \cdot s_3) \cdot q^{n+1}_{i+\frac{1}{2}jk} - \\ -16 \cdot s_3 \cdot q^{n+1}_{i+\frac{1}{2}j-1k} + s_3 \cdot q^{n+1}_{i+\frac{1}{2}j-2k} = B^{n+1}_{i+\frac{1}{2}jk} \quad (10)$$

where $s_3 = \dfrac{\tau}{24 \cdot \mathrm{Re} \cdot \Delta x_3^2}$

The equation (10) is solved by the cyclic penta - diagonal matrix method, the result of which the $q^{n+1}_{i+\frac{1}{2}jk}$ is found.

Once we have determined the value $q^{n+1}_{i+\frac{1}{2}jk}$ we find $\hat{u}_1{}^{n+1}_{i+\frac{1}{2}jk}$:

$$\hat{u}_1{}^{n+1}_{i+\frac{1}{2}jk} = q_{i+\frac{1}{2}jk} + u_1{}^{n}_{i+\frac{1}{2}jk}$$

The velocity components $\hat{u}_2{}^{n+1}_{ij+\frac{1}{2}k}$ and $\hat{u}_3{}^{n+1}_{ij+\frac{1}{2}k}$ are found similarly.

At the second stage the Poisson equation is solved, which is satisfies the continuity equation with considering the velocity field from the first stage. The Poisson equation is translated from the physical space into the phase space by using a Fourier transform and solved with using spectral method.

To solve the three-dimensional Poisson equation is used the Fourier transform, which consists of several steps. The resulting intermediate velocity field does not satisfy the continuity equation. The exact expression for the new velocity field is obtained by adding to the intermediate field the term corresponding to the pressure gradient:

$$u_1^{n+1} = \hat{u}_1^{n+1} - \tau \frac{\partial p}{\partial x_1};$$

$$u_2^{n+1} = \hat{u}_2^{n+1} - \tau \frac{\partial p}{\partial x_2};$$

$$u_3^{n+1} = \hat{u}_3^{n+1} - \tau \frac{\partial p}{\partial x_3}.$$

Substituting the data in the continuity equation and carrying out the transformation, we obtain the Poisson equation for the pressure field:

$$\frac{\partial^2 p}{\partial x_1^2} + \frac{\partial^2 p}{\partial x_2^2} + \frac{\partial^2 p}{\partial x_3^2} = \frac{1}{\tau}\left(\frac{\partial \hat{u}_1^{n+1}}{\partial x_1} + \frac{\partial \hat{u}_2^{n+1}}{\partial x_2} + \frac{\partial \hat{u}_3^{n+1}}{\partial x_3} \right).$$

The equation for pressure is approximated at the point i, j, k takes the following form:

$$\frac{P_{i+1jk} - 2P_{ijk} + P_{i-1jk}}{\Delta x^2} + \frac{P_{ij+1k} - 2P_{ijk} + P_{ij-1k}}{\Delta y^2} + \frac{P_{ijk+1} - 2P_{ijk} + P_{ijk-1}}{\Delta yz^2} = F_{ijk} \quad (11)$$

$$F_{i,j,k} = \frac{1}{\tau}\left(\frac{\hat{u}_1^{n+1}{}_{i+\frac{1}{2},j,k} - \hat{u}_1^{n+1}{}_{i-\frac{1}{2},j,k}}{\Delta x_1} + \frac{\hat{u}_2^{n+1}{}_{i,j+\frac{1}{2},k} - \hat{u}_2^{n+1}{}_{i,j-\frac{1}{2},k}}{\Delta x_2} + \frac{\hat{u}_3^{n+1}{}_{i,j,k+\frac{1}{2}} - \hat{u}_3^{n+1}{}_{i,j,k-\frac{1}{2}}}{\Delta x_3} \right)$$

Pressure P_{ijk} in the physical space goes into the next phase using next dysfunctional:

$$P_{ijk} = \sum_{k_3}\sum_{k_2}\sum_{k_1} \hat{p}(k_1,k_2,k_3) \times e^{\mathrm{I}(\frac{2\pi i k_1}{N_1} + \frac{2\pi j k_2}{N_2} + \frac{2\pi k k_3}{N_3})} \tag{12}$$

$$F_{ijk} = \sum_{k_3}\sum_{k_2}\sum_{k_1} \hat{F}(k_1,k_2,k_3) \times e^{\mathrm{I}(\frac{2\pi i k_1}{N_1} + \frac{2\pi j k_2}{N_2} + \frac{2\pi k k_3}{N_3})} \tag{13}$$

Boundary conditions are taken as periodic for Poisson equation. For solving Poisson equation we use spectral method in combination with Fourier transform. Substituting (12) and (13) expressions in equation (11) and performing transformation in the end we get:

$$\hat{p}(k_1,k_2,k_3) = \frac{\hat{F}(k_1,k_2,k_3)}{2\left[\frac{\cos(\frac{2\pi k_1}{N_1}) - 1}{dx^2} + \frac{\cos(\frac{2\pi k_2}{N_2}) - 1}{dy^2} + \frac{\cos(\frac{2\pi k_3}{N_3}) - 1}{dz^2} \right]}$$

At the final stage the inverse Fourier transform is performed to obtain the solution of the Poisson equation. The obtained pressure field with using fast Fourier transform is translated from the phase space to the physical space and used at the third stage for recalculation the final velocity field

Calculation of turbulence characteristics for Taylor-Green vortex problem

To determine the turbulent characteristics in a physical space, it is necessary to average different values in volume. The averaged values will be used to find the turbulent characteristics. The value averaged over the entire calculated area is calculated by the following formula:

$$\langle u_i \rangle = \frac{1}{N_1 N_2 N_3} \sum_{n=1}^{N_1}\sum_{m=1}^{N_2}\sum_{q=1}^{N_3} \left(\overline{u}_i\right)_{n,m,q}.$$

The dissipation rate is calculated by the following formula:

$$\varepsilon = <2\nu S_{ij} S_{ij}> = 2\nu \left[\left\langle \left(\frac{\partial u_1}{\partial x_1} \right)^2 \right\rangle + \left\langle \left(\frac{\partial u_2}{\partial x_2} \right)^2 \right\rangle + \left\langle \left(\frac{\partial u_3}{\partial x_3} \right)^2 \right\rangle + \frac{1}{2}\left\langle \left(\frac{\partial u_1}{\partial x_2} + \frac{\partial u_2}{\partial x_1} \right)^2 \right\rangle + \right.$$
$$\left. + \frac{1}{2}\left\langle \left(\frac{\partial u_1}{\partial x_3} + \frac{\partial u_3}{\partial x_1} \right)^2 \right\rangle + \frac{1}{2}\left\langle \left(\frac{\partial u_2}{\partial x_3} + \frac{\partial u_3}{\partial x_2} \right)^2 \right\rangle \right]$$

The turbulent kinematic energy is found in the following way:

$$E_k = \frac{1}{2}\left(\left\langle u_1^2 \right\rangle + \left\langle u_2^2 \right\rangle + \left\langle u_3^2 \right\rangle\right) = \frac{3}{2}\left\langle u_1^2 \right\rangle$$

Numerical modelling results. The numerical model allowed to describe the isotropic turbulence decay based on hybrid methods, using finite-difference methods in combination with cyclic penta-diagonal for solving equation of motion and spectral methods is used for solution of Poisson equation.

For this task, the characteristic values of the velocity and length were taken equal to $U_0 = 1$, and $L = 1$ respectively. The calculation grid 128×128×128 was taken. The Reynolds numbers $\mathrm{Re} = \frac{U_0 L}{\nu(2\pi)}$ were taken: 1) $\mathrm{Re} = 100$; 2) $\mathrm{Re} = 300$; 3) $\mathrm{Re} = 600$. In the Table 1 were set up parametres for the comparison of the obtained results of simulation with analytical sollution of vortex problem Taylor –Green.

Initial parametres for Taylor-Green vortex problem	**Initial parametres for this simulation problem**
$L_B = 2\pi$	$L_B = 1$
$a = \frac{2\pi}{L_B} = 1$	$a = \frac{2\pi}{L_B} = 2\pi$
$\mathrm{Re} = \frac{U_0}{\nu a} = \frac{U_0 L_B}{\nu(2\pi)} = 300$	$\mathrm{Re} = \frac{U_0}{\nu a} = \frac{U_0 L_B}{\nu(2\pi)} = 300$
$\nu = \frac{U_0 L_B}{(2\pi)\mathrm{Re}} = \frac{1}{\mathrm{Re}}$	$\nu = \frac{U_0 L_B}{(2\pi)\mathrm{Re}} = \frac{1}{(2\pi)\mathrm{Re}}$
$dt = 0.01 = \frac{dx}{U_0} CFL = \frac{2\pi}{64} CFL$	$dt = \frac{dx}{U_0} CFL = \frac{0.10185916}{64} CFL$
$T = aU_0 t = \frac{2\pi U_0 t}{L_B}$	$T = aU_0 t = \frac{2\pi U_0 t}{L_B}$
$k(t=0) = \frac{1}{8} U_0^2 = 0.125d0$	$k(t=0) = \frac{1}{8} U_0^2 = 0.125d0$
$\varepsilon(t=0) = \frac{3}{4}\nu U_0^2 a^2 = \frac{0.75}{\mathrm{Re}}\left(\frac{2\pi}{L_B}\right)^2$	$\varepsilon(t=0) = \frac{3}{4}\nu U_0^2 a^2 = \frac{0.75}{2\pi\,\mathrm{Re}}\left(\frac{2\pi}{L_B}\right)^2$

Table 1. The preset parameters for the comparison results of exact solution with numerical solution of vortex problem Taylor –Green

As the results of the simulation with different Reynolds numbers, the following turbulence characteristics were compared with analytical solution of Taylor –Green vortex problem: kinetic energy and dissipation rate of turbulent flow. Fig. 1 presents the comparison of the turbulent kinetic energy obtained in this work with the analytical solution obtained on the basis solution of Taylor –Green vortex problem at different Reynolds numbers: 1) $\mathrm{Re} = 100$; 2) $\mathrm{Re} = 300$; 3) $\mathrm{Re} = 600$. The obtained results shows the satisfactory agreement up to $T = 3$.

Presented in Fig. 2 the matching results of the dissipation rate of turbulence decay over the time received in this numerical simulation with exact solution of Taylor –Green vortex problem at different Reynolds number shows good agreement till $T = 1.5$, because the order of accuracy in time is $O(t^3)$.

In the simulation results, the average error between analytical and numerical solutions was defined, and it was equal to $\varepsilon_{err} = 10^4$.

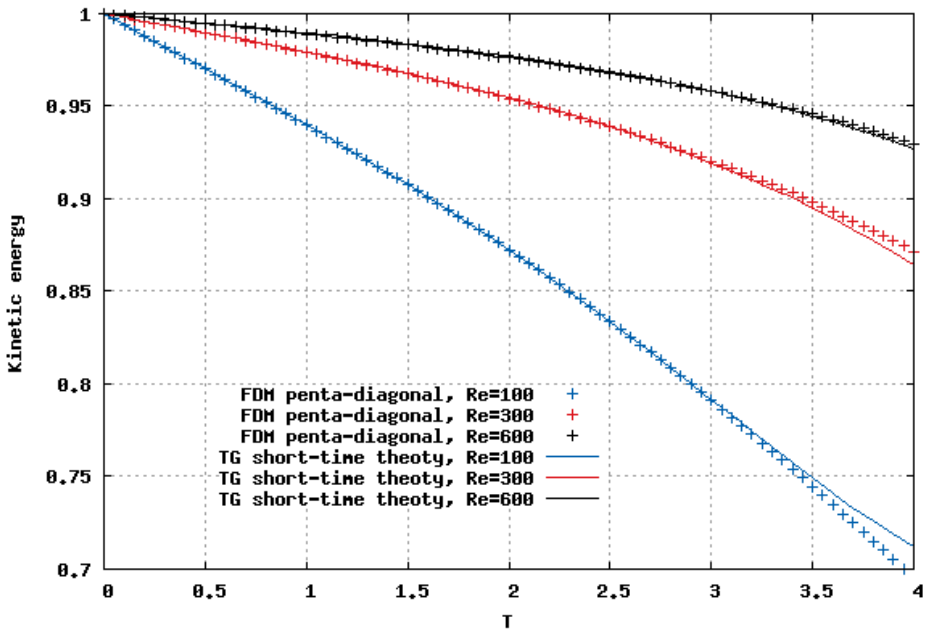

Figure -1. Comparison simulation result of the evolution of kinetic energy over the time with direct methods of Taylor –Green vortex at different Reynolds number.

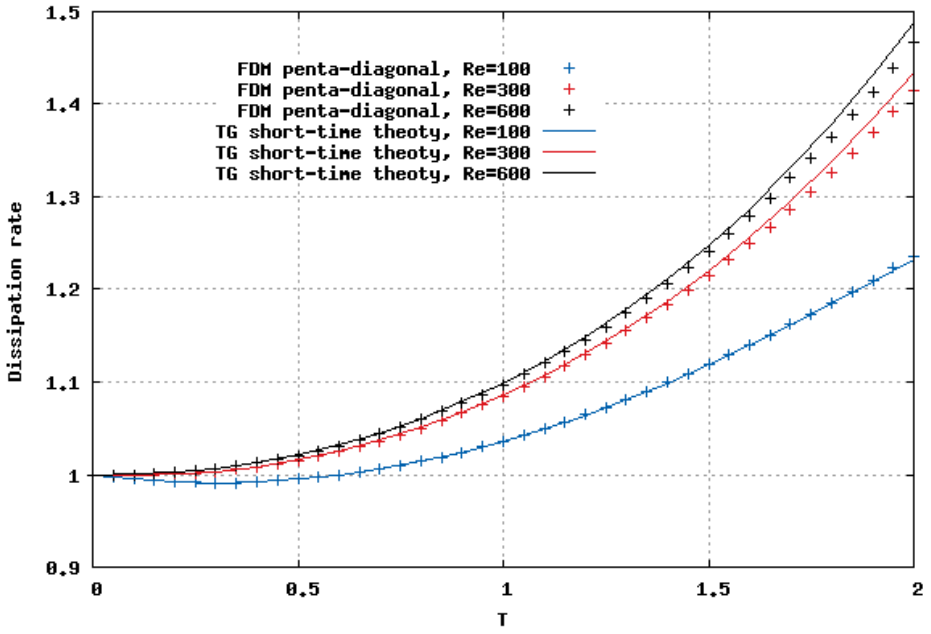

Figure -2. Comparison simulation result of the dissipation rate of turbulence decay over the time with direct methods of Taylor –Green vortex at different Reynolds number.

Conclusion

The numerical algorithm for solving non-stationary three-dimensional Navier-Stokes equations for modelling of isotropic turbulence decay with using hybrid methods: finite-difference and spectral methods with high order of accuracy and the efficiently algorithm for parallelization at different Reynolds numbers is developed. The using the finite-difference methods in combination with cyclic penta-diagonal matrix for solution of motion equation allowed to reach high order of accuracy and using spectral methods for solution of Poisson equation, makes it possible to gain the time in computation. For validation of the given algorithm the classical problem of Taylor and Green with intial parametres for modeling of isotropic turbulence decay was solved. Thus, the numerical simulation results in obtaining turbulence characteristics show good agreements with analytical solution and the average error $\varepsilon_{err} = 10^4$ between analytical and numerical solutions was defined.

Thus, the developed numerical algorithm can be used for simulation of the formation and dynamics of clouds with considering the turbulent processes.

This research was performed in the framework of the project "Development of software for modeling the dynamics of clouds formed at ground explosion of the launch vehicle".

Acknowledgements. This research was supported by 0383/GF4. We thank professor Lian-Ping Wang for discussions.

References

[1] Taylor, G.I., Green, A.E., (1937), “Mechanism of production of small eddies from large ones”, *Proceedings of the royal society, Mathematics and physical sciences,* Vol. 158 № 895, pp. 499-521.

[2] Brachet, M. E., Meiron, D. I., Orszag, S. A., Nickel, B.G., Morf, R.H., Frisch, U. (1983), “Small-scale structure of the Taylor-Green vortex”, *J.Fluid Mech.* Vol.130, pp.411-452.

[3] Brachet, M.E. (1991), “Direct simulation of three – dimensional turbulence in the Taylor – Green vortex”, *J. Fluid Dynamics Research*, Vol. 8, pp. 1-8.

[4] DeBonis, J. R. (2013), “Solutions og the Taylor-Green vortex problem using high – resolution explicit finite difference methods”, NASA / TM -2013-217850. pp. 1-28.

[5] Kim, J., Moin, P. (1985), “Application of a fractional – step method to incompressible Navier- Stokes equations”, *J. Comp. Phys.* Vol.59, pp.308-323.

[6] Navon, M. (1987), “Pent: A periodic pentadiagonal systems solver”, *J. Communications in applied numerical methods*, Vol.3, pp. 63-69.

GENERALIZED LIPPMANN-SCHWINGER EQUATION FOR INITIAL BOUNDARY VALUE PROBLEM IN 3D BLOCKY MULTIPHYSICS MULTI-SCALE MEDIA

Alena A. Ayzenberg[1,*], Arkady M. Aizenberg[2], Morten Jakobsen[3]

[1]University of Bergen, alena.ayzenberg@uib.no

[2]Institute of Petroleum Geology and Geophysics SB RAS, aizenbergam@ipgg.sbras.ru

[3]University of Bergen, morten.jakobsen@uib.no

1. Introduction

It is known that the conventional Lippmann-Schwinger equation is commonly used for solving of wave motion problems in monophysics media such as acoustic, elastic, electromagnetic, optic etc. media with inclusions [1]. In multiphysics blocky media, for example: combination of solid with porous media (as salt structures with porous fluid-saturated reservoirs), the Lippmann-Schwinger equation needs to be generalized for blocky model case. For this, we suggest to use TPOT (the Transmission-Propagation Operator Theory) [2]. The generalized equation can be then used for solving of wave motion problems in the general 3D multiphysics multi-scale blocky media case with curved interfaces. Since this generalized equation has a similar structure to the conventional one, its solution can be done by any of the existing solvers, both numerical and analytical.

2. The generalized Lippmann-Schwinger equation for 3D blocky multiphysics multi-scale media

We consider the IBVP (initial boundary value problem) system of wave motion equations for medium with M blocks with a source in the 1st block [2, 3]

$$\left[\mathbf{D}_{\mathbf{x}} + \mathbf{M}(\omega)\right]\mathbf{u} = \mathbf{f} \ , \tag{1}$$

where $\mathbf{u}$ is the wavefield, $\mathbf{f}$ is the source function, $\mathbf{D}_{\mathbf{x}}$ is the differential operator and $\mathbf{M}$ is the medium parameters (this matrix for different media is given in [4, 5]) operator and ω is angular frequency. The wave vector $\mathbf{u}$ satisfies the interface conditions. Equation (1) in the wave amplitude form is [2, 3]

$$\mathbf{a} = \mathbf{L}\,\mathbf{a} + \mathbf{a}^{(0)} \ , \quad \mathbf{L} = \mathbf{P}\,\mathbf{T} \ , \tag{2}$$

where $\mathbf{a}^{(0)}$ is the feasible source wavefield [6], $\mathbf{T}$ is the transmission (reflection/refraction) operator and $\mathbf{P}$ is the propagation operator. The solution is represented as [2, 3]

$$\mathbf{a} = \left[\mathbf{P}\,\mathbf{T}\right]^{N+1}\mathbf{a} + \left\{\sum_{n=0}^{n=N}\mathbf{a}^{(n)}\right\}, \quad \mathbf{a}^{(n)} = \mathbf{P}\,\mathbf{T}\,\mathbf{a}^{(n-1)} \quad n = \overline{1,N} \ , \tag{3}$$

$$\mathbf{a} = \lim_{N\to\infty}\left\{\sum_{n=0}^{n=N}\mathbf{a}^{(n)}\right\}, \quad \lim_{N\to\infty}\left\{\left[\mathbf{P}\,\mathbf{T}\right]^{N+1}\mathbf{a}\right\} = \mathbf{0} \ , \tag{4}$$

where $\mathbf{a}^{(n)}$ is n times transmitted (reflected/refracted) wavefield. Let us introduce a local perturbation of the medium. Equation (2) for the reference medium has the form

$$\mathbf{a}_0 = \mathbf{L}_0\,\mathbf{a}_0 + \mathbf{a}^{(0)} \ , \tag{5}$$

where

$$\mathbf{L} = \mathbf{L}_0 + \delta\mathbf{L} \ , \quad \mathbf{a} = \mathbf{a}_0 + \delta\mathbf{a} \ . \tag{6}$$

We notice that the perturbed operator $\delta\mathbf{L} \neq \mathbf{O}$ inside the local support only. Outside the local support $\delta\mathbf{L} \equiv \mathbf{O}$. Also notice that $\delta\mathbf{a} \neq \mathbf{0}$. Substituting equation (2) in (5), we obtain

$$\left(\mathbf{I}-\mathbf{L}\right)\mathbf{a} = \left(\mathbf{I}-\mathbf{L}_0\right)\mathbf{a}_0 \ . \tag{7}$$

Substituting (6) in (7), we obtain

$$\left(\mathbf{I}-\mathbf{L}_0\right)\mathbf{a} = \left(\mathbf{I}-\mathbf{L}_0\right)\mathbf{a}_0 + \delta\mathbf{L}\,\mathbf{a} \ . \tag{8}$$

Since $\left\|\mathbf{L}_0\right\| < 1$ [2, 3, 6], we multiply equation (8) by $\left(\mathbf{I}-\mathbf{L}_0\right)^{-1}$ from the left and derive the Lipmann Schwinger equation in the general form

$$\mathbf{a} = \mathbf{a}_0 + \left(\mathbf{I}-\mathbf{L}_0\right)^{-1}\delta\mathbf{L}\,\mathbf{a} \ . \tag{9}$$

If one wishes to obtain the scattering T-operator [7] for equation (9), it could be done as following. Multiplying (9) by $\delta\mathbf{L}$ from the left, we get

$$\delta\mathbf{L}\,\mathbf{a} = \delta\mathbf{L}\,\mathbf{a}_0 + \delta\mathbf{L}\left(\mathbf{I}-\mathbf{L}_0\right)^{-1}\delta\mathbf{L}\,\mathbf{a} \ . \tag{10}$$

Notice that $\delta\mathbf{L}\,\mathbf{a} \neq \mathbf{0}$ inside the local support. Solving equation (10) with respect to $\delta\mathbf{L}\,\mathbf{a}$, we obtain

$$\delta\mathbf{L}\,\mathbf{a} = \left[\mathbf{I}-\delta\mathbf{L}\left(\mathbf{I}-\mathbf{L}_0\right)^{-1}\right]^{-1}\delta\mathbf{L}\,\mathbf{a}_0 \ . \tag{11}$$

In formula (11) we can introduce a T-operator as it was done in [7]

$$\delta\mathbf{L}\,\mathbf{a} = T\,\mathbf{a}_0 \tag{12}$$

with the generalized T-operator by formula

$$T = \left[\mathbf{I}-\delta\mathbf{L}\left(\mathbf{I}-\mathbf{L}_0\right)^{-1}\right]^{-1}\delta\mathbf{L} \ . \tag{13}$$

This operator generalizes T-operator from [7].

3. Conclusions

This work suggests a generalization of the classical Lippmann-Schwinger equation by TPOT. While the classical equation is used for wave motion problems in monophysics media, the new equation can be used for 3D blocky multiphysics media combining different media, for example: salt structures with porous fluid-saturated reservoirs.

References

[7] Bonnet, M., 2016. Solvability of a volume integral equation formulation for anisotropic elastodynamic scattering, J. Int. Eq. Appl. 28, 2, 169-203.
[8] Aizenberg, A.M., Zyatkov, N.Y., Ayzenberg, A.A., Rakshaeva, E.Z., 2014. New concepts of the transmission-propagation operator theory in seismic diffraction modeling and interpretation, Extended Abstracts, 76th EAGE Conference, We-P06-07.
[9] Ayzenberg, A.A., 2015. Transmission-Propagation Operator Theory and Tip-Wave Superposition Method for sub-salt shadow wavefield description, Ph.D. thesis, Norwegian University of Science and Technology.
[10] Wapenaar, K., Fokkema, J., 2004, corrected 2010. Reciprocity theorems for diffusion, flow and waves, J. Appl. Mech. 71 145–150.
[11] Wapenaar, K., Douma, H., 2012. A unified optical theorem for scalar and vectorial wave fields, J. Acoust. Soc. Am. 131 (5) 3611–3626.
[12] Aizenberg, A.M., Ayzenberg, A.A., 2015. Feasible fundamental solution of the multiphysics wave equation in inhomogeneous domains of complex shape, Wave Motion, 53, 66-79.
[13] Jakobsen, M., Ursin, B., 2015. Full waveform inversion in the frequency domain using direct iterative T-matrix methods, J. Geophys. Eng., 12, 400–418.

TPOT&TWSM FOR 3D MULTIPHYSICS MULTI–SCALE MODELS WITH COMPLEX INTERFACES. UU-MODEL SOLUTION SEPARATION

Alena A. Ayzenberg[1,*], Nikolay Zyatkov[2], Arkady M. Aizenberg[3]

[1]University of Bergen, alena.ayzenberg@uib.no

[2]Novosibirsk State University, nikolay.zyatkov@gmail.com

[3]Institute of Petroleum Geology and Geophysics SB RAS, aizenbergam@ipgg.sbras.ru

4. Introduction

There are various physical and numerical methods allowing appropriate modeling of multiphysics wavefields in multiscale effective models, for example: metal processing, composite material, oil and gas development, geophysical imaging and interpretation, fuel cell technology, biomedical tissue engineering etc. We propose TPOT&TWSM (the pure analytical Transmission-Propagation Operator Theory and its software package - the Tip-Wave Superposition Method).

5. TPOT&TWSM technology for IBVP solution

IBVP is conventionally formulated in terms of the kinematic and dynamic fields. TPOT [1] rewrites IBVP statement in terms of the multiphysics wave theory: unknown wave vector $\mathbf{a}$ in form of p_m wave amplitudes $\mathbf{a}^{\pm}_{mn} = \left(a^{\pm}_{mn1} \quad \dots \quad a^{\pm}_{mn\,p_m}\right)^T$ counter-propagating at n-th interface of m-th domain and IBVP in form of the transmission-propagation integral equation (TPIE) $\mathbf{a} = \mathbf{TP}\,\mathbf{a} + \mathbf{a}^{(1)}$. Here, $\mathbf{a}^{(1)} = \mathbf{T}\,\mathbf{a}^{(0)}$ is the single transmitted wavefield, $\mathbf{a}^{(0)} = \sum_{n=0}^{N} \mathbf{a}^{[n]}$ is the source wavefield, $\mathbf{a}^{[0]}$ is the conventional spherical wave and $\sum_{n=1}^{N} \mathbf{a}^{[i]}$ is the total diffraction at the boundary [2]. The transmission operator $\mathbf{T}$ contains the generalized plane-wave transmission(reflection/refraction) coefficients. The propagation operator $\mathbf{P}$ in domains contains the polarization matrix and the feasible Kirchhoff-type surface integral operator accounting for the total diffraction [2]. The total solution is $\mathbf{a} = \left[\mathbf{T}\,\mathbf{P}\right]^{N+1} \mathbf{a} + \sum_{n=1}^{N} \mathbf{a}^{(n)}$ with n-tuple transmitted wavefields $\mathbf{a}^{(n)} = \mathbf{T}\,\mathbf{P}\,\mathbf{a}^{(n-1)}$ for $n \geq 2$. TWSM and highly-optimized TWSM [3] compute TPOT solutions $\mathbf{a}^{(n)}$ on a GPU cluster by approximation of operator $\mathbf{TP}$ by nonsparse matrix. TWSM is valid in the multiscale range $10 \leq h/\lambda_{dom} \leq 99$, where h and λ_{dom} are model size and dominant wavelength. TPOT&TWSM was compared with canonical analytical solutions [4], laboratory data [5] and numerical methods [6].

6. UU- model solution separation: the creeping wave

Figures 1 and 2 give a UU-model and an auxiliary W-model. Figure 3a-e illustrates $\mathrm{a}^{[0]}$, $\mathrm{a}^{[1]}$, $\mathrm{a}^{[2]}$, $\mathrm{a}^{[3]}$ and $\mathrm{a}^{(0)}$ for UU-model where the terms of the 4th and higher order are negligibly small. Figure 4 gives $\mathrm{a}^{(0)}$ for W-model from [3]. Figure 5 represents the difference seismogram for UU- and W-models, which is the creeping wave occurring at curved boundary parts of UU-model and not occurring at the flat faces of W-model.

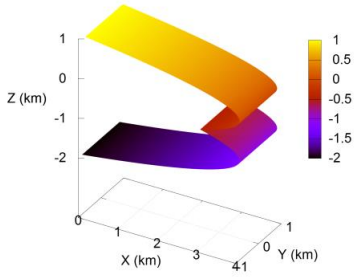

Figure 1. UU-model

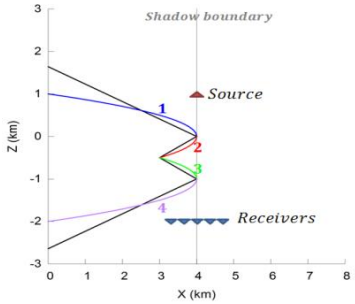

Figure 2. 2D cross-sections UU- and W-models

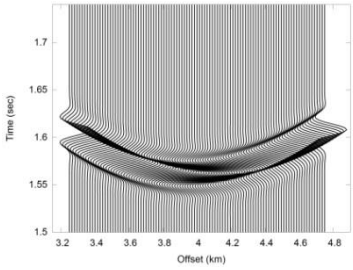

Figure 3a. UU-model: $a^{[0]}$

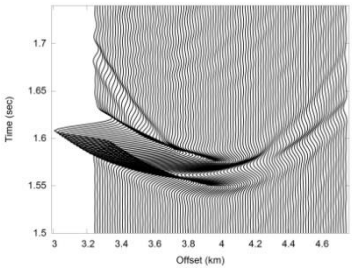

Figure 3b. UU-model: $a^{[1]}$

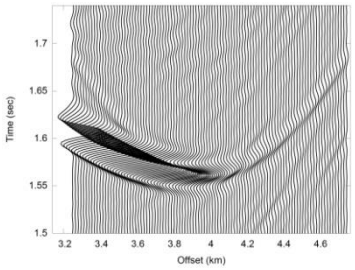

Figure 3c. UU-model: $a^{[2]}$

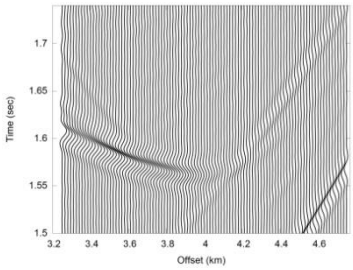

Figure 3d. UU-model: $a^{[3]}$

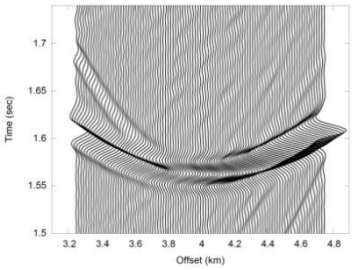

Figure 3e. UU-model: $a^{(0)}$

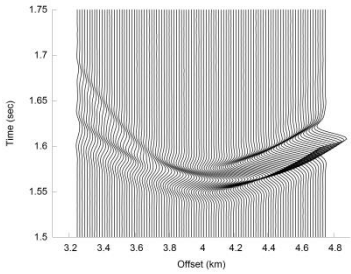

Figure 4. W-model: $a^{(0)}$ [3]

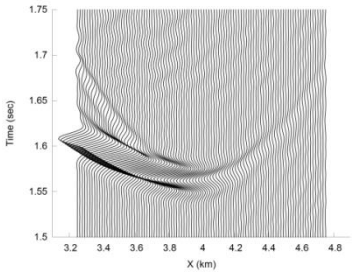

Figure 5. Difference UU-W

7. Conclusions

TPOT&TWSM does the solution separation for 3D multi-physics multi-scale media with curved interfaces. UU-model solution separation demonstrated the creeping wave.

References

[14] Aizenberg, A.M., Zyatkov, N.Y., Ayzenberg, A.A., Rakshaeva, E.Z., 2014. New concepts of the transmission-propagation operator theory in seismic diffraction modeling and interpretation, Extended Abstracts, 76th EAGE Conference, We-P06-07.

[15] Aizenberg, A.M., Ayzenberg, A.A., 2015. Feasible fundamental solution of the multiphysics wave equation in inhomogeneous domains of complex shape, Wave Motion, 53, 66-79.

[16] Zyatkov, N., Ayzenberg, A., Aizenberg, A.M., Romanenko A., 2013. Highly-optimized TWSM algorithm for modeling cascade diffraction in terms of propagation-absorption matrices, Extended Abstracts, 75th EAGE Conference, Th-P02-11.

[17] Ayzenberg, A., Zyatkov, N., Stovas, A., Aizenberg, A.M., 2014. The feasible near-front wavefield below salt overhang in terms of cascade diffraction, Extended Abstracts, 76th EAGE Conference, We-P06-06.

[18] Tantsereva, A., Ursin, B., Favretto-Cristini, N., Cristini, P., Aizenberg, A.M., 2014. Numerical modeling of three-dimensional zero-offset laboratory data by a discretized Kirchhoff integral, Geophysics, 77 (2), T77-T90.

[19] Ayzenberg, A.A., Weibull, W., Zyatkov, N., Aizenberg, A.M., Stovas, A., 2015. Comparison TWSM with FD, APSLIM Workshop Meeting. Loucen Castle, Czech Republic.